Strain behavior of geogrids reinforcing sand under a rectangular footing

Raid R. Al-Omari [i], Zeyad S. M. Khaled [ii] and Tawfek Sheer Ali [iii]

i) Professor of Geotechnical Engineering, Department of Civil Engineering, College of Engineering, Al-Nahrain University, Baghdad, Iraq, tosharaid@yahoo.com
ii) Assistant Professor of Construction Management, Department of Civil Engineering, College of Engineering, Al-Nahrain University, Baghdad, Iraq, zeyadsmkhalid@yahoo.com
iii) Assistant Lecturer, Department of Civil Engineering, College of Engineering, Kufa University, Najaf, Iraq, PhD researcher in Al-Nahrain University, Baghdad, Iraq, tawfeeq76@gmail.com

ABSTRACT

An experimental study of the strain behavior of high strength geogrids used to reinforce sandy soil under a 60 x 230 mm rectangular footing is conducted. The effect of two types of geogrids on the bearing capacity of the composite is investigated as well. Three layers of Netlon CE121 and Tensar SS2 geogrids were used. The first layer was positioned at 0.25B below the footing base while the third layer at a depth of B below the base where B is the footing width. The main aim of the study is to measure the strain and elongation occurring in the ribs of Tensar SS2 geogrid. The peak tensile strength of Tensar SS2 geogrid MD/XMD is 14.4/28.2 kN/m and it is 6.4 kN/m for Netlon CE121. TML strain gauges and other compatible accessories are used. The sand is statically loaded; the relative density was 71.8 % using a raining technique. It is found that the use of geogrids produces a bearing capacity ratio of reinforced to unreinforced sand of 2.35 and 2.9 for Netlon CE121 and Tensar SS2 respectively. The results revealed also that the measured strain and elongation in the ribs decrease as the depth of geogrid layers increases and as the horizontal distance from the footing centre increases as well. The strain in geogrid ribs practically diminishes at a depth of about the width of footing (B) and at a horizontal distance of about 2.33B from the centerline of footing. A maximum rib strain of about 0.0001 was measured corresponding to a maximum footing bearing stress of 363 kN/m^2.

Keywords: sand, geogrid strain, bearing capacity, physical model

1 INTRODUCTION

The term *reinforced soil* describes any soil mass which has its shear strength improved by combining it with resisting elements; these resisting elements, or reinforcement may take the form of bars, strips, tubes, grid or sheets. The observed increase in soil shear strength of a reinforced soil is always a direct result of relative soil-reinforcement displacement (Pedley, 1990).

Al-Omari et al. (1987) used perforated steel discs and the plastic geomesh Netlon CE121 as reinforcing materials to investigate the relation of interlocking mechanism to the aperture size (T) of the geogrid mesh. The ratio of the aperture size in the steel mesh to the grain size of the sand D_{50} was varied in the test but the area of holes to the area of solid is kept constant in each disc. The conclusions were that the strength enhancement in mesh reinforced sand depends on the mechanism of interlocking which is in turn affected by the ratio of aperture size to particle diameter. The peak stress ratio (σ_1/σ_3) of mesh reinforced sand increases to a maximum at $T/D_{50} \approx 13.5$ and then drops beyond this value. The use of plastic mesh with the appropriate stiffness and the appropriate aperture size makes the strength of the sand approximately independent of the sand density.

Shin and Das (2000) conducted small-scale laboratory model tests on surface and shallow strip foundation supported by sand reinforced with multiple layers of geogrid. Based on the test results, for a given thickness of the reinforcement zone the bearing capacity ratio increases when the depth of the foundation is greater than zero.

Study of strain mobilizing in polyester and steel grid reinforcement were carried out but using large scale direct shear tests (Bergado et al. 2012). Chen (2007) measured the strains occurring in high strength geogrids during model bearing capacity tests. However he reported results of both bearing capacity and strains which are too exaggerated (Fakhraldin 2013).

2 MATERIALS AND TESTING

2.1 Materials

The properties of the used soil are shown in Table 1. Sieve analysis is conducted to characterize the soil grain size distribution according to ASTM (D422-2007) as shown in Fig. 1. The soil is classified as *SP* type (*Poorly graded sand*) according to the Unified Soil Classification. ASTM (D4253-2007) and ASTM (D4254-2007) were implemented to find the maximum

and minimum dry unit weight. A raining technique is used to fill the box of test at a relative density larger than 70%, using special equipment as shown in Fig. 2. The porosity was measured by placing 6 cylindrical density pots to collect the sand under the moving hopper. The pots are 80 mm in height and 80 mm in diameter measured from inside. A pot diameter larger than 3 inches is used to satisfy the requirement of free fall method (Kolbuszewski, 1948). The deposited sand was carefully collected using the pots with the excess sand removed to keep top surface leveled. The pots are then weighted, and by knowing the specific gravity, the porosity could be calculated. The calibration was conducted twice for the second and third layer before starting the test. The drop height was chosen as 800 mm to give a placing density of 16.7 kN/m^3 which is equivalent to the working void ratio e = 53.9%. Porosity and relative density were evaluated to be 53% and RD = 71.8% respectively. The weight of every empty pot was measured using a sensitive balance and the volume of pots was accurately determined by measuring the weight required to fill each pot. The air dried sandy soil was placed in the box according to the raining technique, the thickness of each layers was 200 mm. After each test, the sand box should be completely emptied.

A Triaxial test is performed to estimate the angle of internal friction and cohesion of soil. The angle of internal friction Øº is found to be 40º at peak stress level and the cohesion is zero.

The loading frame and the required accessories are shown in Fig. 3.

Netlon CE121 and Tensar SS2 geogrids are used. The peak tensile strength of Tensar SS2 geogrid MD/XMD is 14.4/28.2 kN/m and it is 6.4 kN/m for Netlon CE121.

TML strain gauges, SB tape and compatible adhesive type CN, shown in Fig. 4, is used to measure the strain occurring in the ribs of geogrid.

Table 1. The Properties of Soil.

G_s	2.62
$Ø_{used}$	40º
$R_{D\ used}$	71.8%
O.M.C	9.8%
D_{60} D_{50} D_{30} D_{10}	0.6 mm 0.5 mm 0.3 mm 0.2 mm
C_u	3.5
C_c	0.9

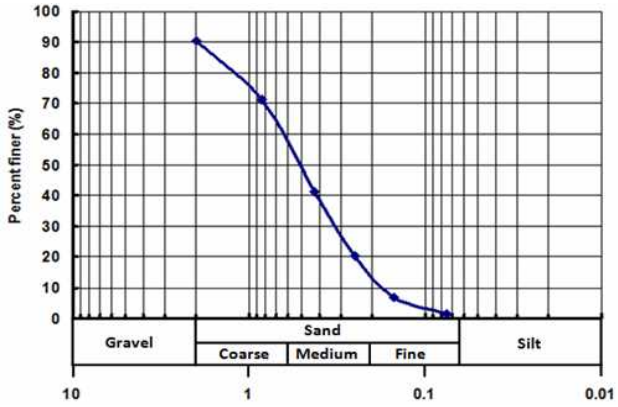

Fig. 1. Grain size distribution of soil.

Fig. 2. Soil raining equipment

Fig. 3. Loading frame and required accessories

Fig. 4 TML strain gauges, SB tape and compatible adhesive CN

2.2 Model Configuration

The model is prepared as shown in Fig. 5. The footing model is placed on the top of the soil surface in the model test box. The first layer of geogrids is placed at a depth of (u) equals to 0.25B. The leftover depth is divided into two intervals, each of 0.375B. The footing length to breadth ratio was 3.83; side wall lubrication and wide tank were employed. The tank dimensions are 500 mm × 600 mm × 1000 mm in width, height and length respectively, footing dimensions are 60 mm × 230 mm in width and length respectively.

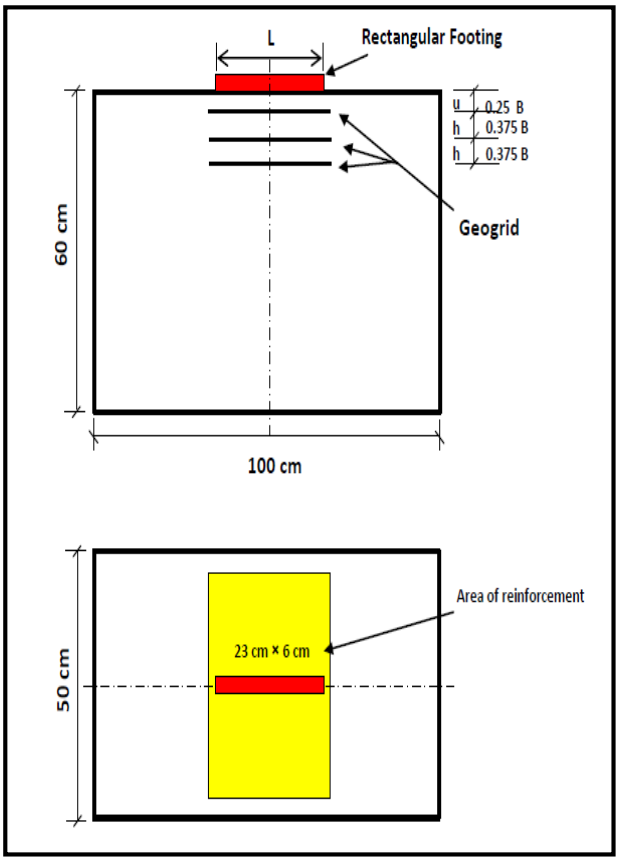

Fig. 5 Geometry and top plan of the geogrid and footing model.

2.3 The Datatronic 128-channel Automatic Data Acquisition System

All data collection takes place automatically using the Datatronic 128-channel automatic data acquisition system. A Windows based program with menu driven command selection is straightforward and easy to follow. The device is capable of acquiring inputs from any type of transducer: Strain Gauge Bridge, LVDT (Linear Variable Differential Transformer) with optional adapter and Potentiometer. A continual live display of test diagrams is provided in addition to test data exportation with TXT files for consecutive processes, with Excel or other SW. A personalized printout of certificates and test diagrams is available. System configuration is facilitated by a 5 key membrane keyboard with encoder for rapid setting. Data logging is facilitated by user-friendly software included in the Datatronic package. The system allows setting for each channel the sampling type in linear form, square root form, logarithmic form and personalizable form, with frequencies from very fast (one second) to infinite, without reading limits (storage limits are linked to PC memory), with the possibility of delaying the start time.

The dimensions of the unit are: 460 × 540 × 350 mm and Weight: 12 kg as shown in Fig. 6.

Fig. 6 The datatronic 128-channel automatic data acquisition system

2.4 Calibration Method

The datatronic acquisition system reads the strain through an electric circuit as divisions. The readings were calibrated using single rib of geogrid and the strain gauge was fixed on the middle of the rib and tested by the computer controlled electronic universal testing machine. The strain gauge connected to strain gauge amplifier which by turn connected to the datatronic acquisition system. The computer controlled universal testing machine records the strain against time, the acquisition system records the divisions against the same time. Accordingly a calibration between divisions and strains was carried out and the following equation was obtained with coefficient of determination $r^2 = 0.9689$

$$\epsilon = 5R\ 10^{-8} + 0.0002$$

where

R: is the reading of the acquisition system (divisions).The output reading of the unit is a strain (ε), the elongation (Δl) can be given by multiplying the strain (ε) by the rib length (l).

3 BEARING CAPACITY TESTS RESULTS

3.1 Unreinforced Soil Model Test Results

The footing model test is conducted on the sand alone. The ultimate bearing capacity and load-settlement relation is shown in Fig. 7. The rate of loadings is 1 mm/s as a static loading. The footing was placed on the upper free surface of soil. The value of bearing capacity is considered as a reference to investigate the improvement of soil using the geogrid. From the relationship between bearing pressure and

relative settlement (s/B %) of soil, it can be seen that the obtained ultimate bearing capacity was 123.2 kPa. The relative settlement at the ultimate bearing capacity is 13.3%. The point of ultimate bearing capacity was easily marked on the load-settlement curve since the test is strain-controlled and the peak is clearly visualized.

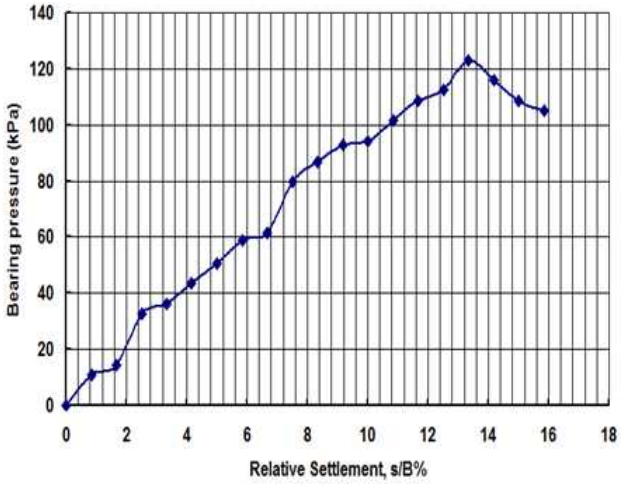

Fig. 7 Bearing pressure versus relative settlement for footing resting on soil alone.

3.2 Reinforced Soil Model Test Results

Tests are performed to study the effect of using geogrids to improve the bearing capacity of soil. Two types of geogrids (Netlon CE121 and Tensar SS2) are used. The relation between the ultimate bearing capacity (q_u) and the relative settlement (s/B%) is plotted as shown in Fig. 8. From the figure it can be seen that Tensar SS2 type gives a higher improvement in bearing capacity than the Netlon CE121. The bearing capacity ratio (BCR) is the ratio of bearing capacity using geogrids to the bearing capacity without geogrid. For Netlon CE121 geogrid, the (BCR) is 2.35 and for Tensar SS2 is 2.9. This is because Tensar SS2 strength is higher than Netlon CE121. The results give indication that higher strength grids yields higher bearing capacity.

4 STRAIN DISTRIBUTION RESULTS

4.1 Strain and Elongation Measurement

On scrutiny of the available literature, it appears that there is little previous work on the straining mechanism occurring in the geogrid ribs during the application of foundation loading where the failure is progressive. The study of strain in the ribs of geogrid was conducted for Tensar SS2 only.

The distribution of strains in the geogrid ribs is important to understand the enhancement mechanism of bearing capacity, to what extent there is a need to high stiffness/strength geogrids, and at which stress level the soil-grid bond may break.

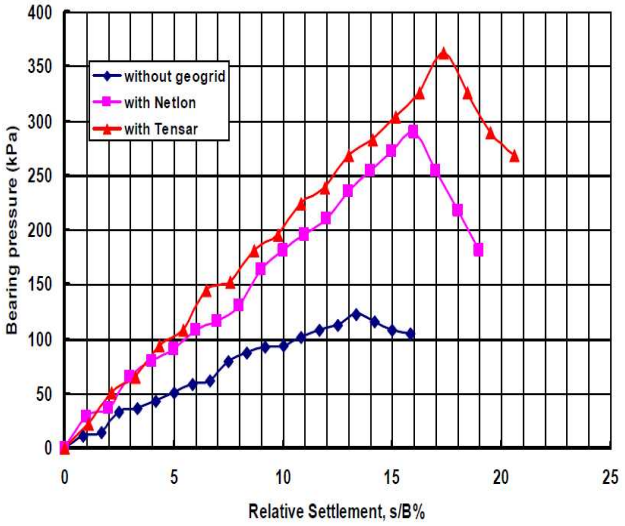

Fig. 8 Bearing pressure versus relative settlement for footing with and without geogrids.

The strain gauges are distributed to cover one side of footing reinforcement because of similarity at both sides. Strain gauges are fixed on the long rib because it has a higher strength and modulus of elasticity than the short rib. The reinforcement sheet was laid on the sand so that the long ribs are perpendicular to the long side of the footing in order to gain higher improvement. Fixing of strain gauges on the ribs of geogrid and the distribution of strain gauges are shown in Fig. 9. Table 2 shows horizontal distances of the strain gauges from the centerline of footing. The same distribution is repeated for the second and third layers. The centerline of the geogrid sheet coincides with the centerline of footing. The spacing between strain gauges was 40 mm except for gauge No.4 where the spacing was increased because the strain distribution is expected to be flattened away from the footing.

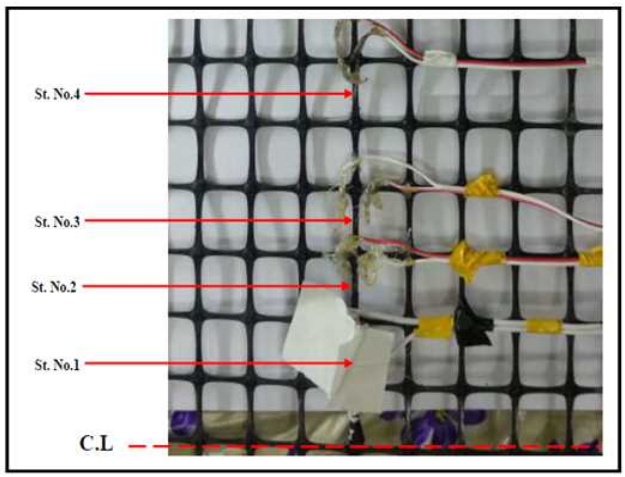

Fig. 9 The distribution of strain gauges on Tensar SS2 reinforcement.

Table 2. Horizontal distances of the strain gauge from the center line of footing.

Strain gauge number	Distance of gauge (d) from the center of footing (mm)	Relative distance (d/B) of gauge from center of footing
1	60	1
2	100	1.67
3	140	2.33
4	220	3.6

4.2 Horizontal and Vertical Strain Distribution

The distribution of strains occurring in strain gauges which are fixed on the geogrid ribs are demonstrated in Fig. 10. The values shown are recorded at the ultimate bearing capacity.

Figure 10 demonstrates the relationship between the horizontal distance, relative distance, and strain. It has been found that the values of strain decrease when the strain gauge distance from the centerline of footing for each layer increase. A maximum rib strain of about 0.0001 was measured corresponding to a maximum footing bearing stress of 363 kN/m^2.

The position of the farthest strain gauge is at a distance of 3.6B, which marked here the distance at which the strain has died out. These findings agree with other researchers, the total distance of 7B including both sides, is almost the zone of stress concentration, (Chen, 2007). However, practically the strains have become insignificant at a distance of 2.33B as may be seen in Fig. 10. This means that a total width of 4.66B is the practical width of stress concentration.

Figure 11 shows the relationship between the horizontal distance, relative distance, and elongation in geogrid ribs. They have the same behavior as in Fig. 10 because of the linear relationship between the strain and elongation.

Figure 12 shows the relationship between the depth of strain gauges which are represented by the depth of geogrid sheet under the footing and the strain. The relationship is drawn for the values of strain at the ultimate bearing capacity. Strain decreases as the depth under footing increases. The values of strain decrease to a small value for the third layer. Practically the depth B may be considered as the depth where the strains become insignificant.

Figure 13 explains the relationship between elongation and depth of strain gauges. The relationships show how the values of elongation vary in each rib of geogrid mesh as the embedment depth increases. The elongation decrease as the depth increases.

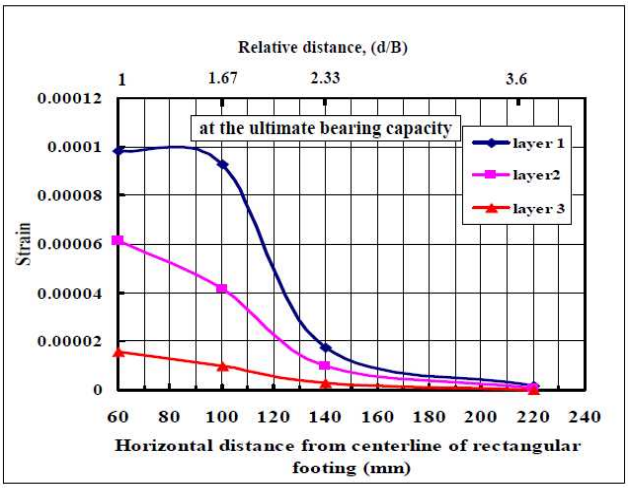

Fig. 10 The relationship between strain and distance from the centerline along the long side of footing.

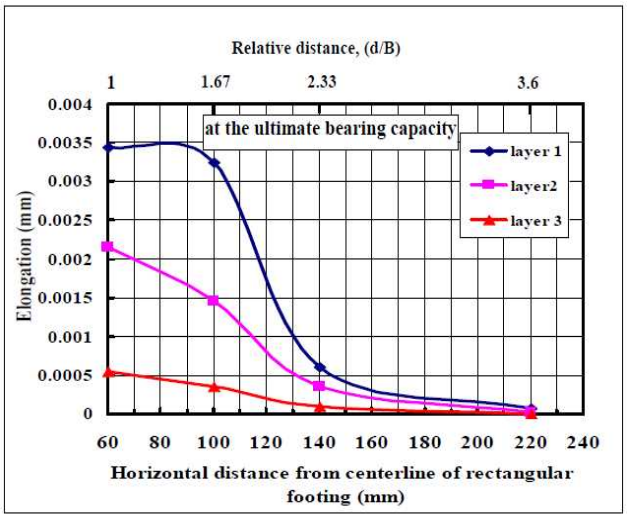

Fig. 11 The relationship between elongation and distance from the centerline along the long side of footing.

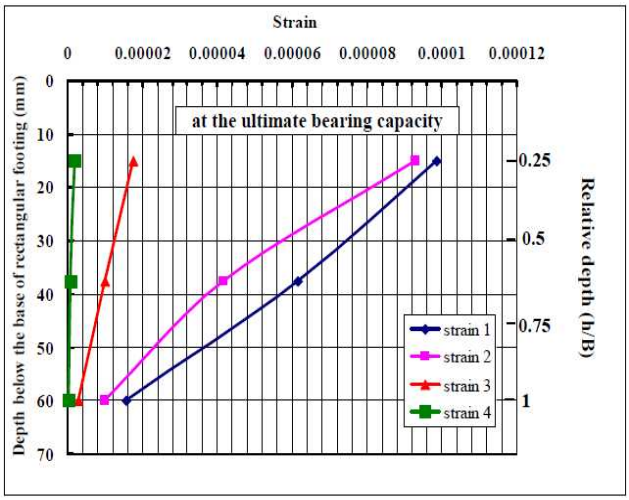

Fig. 12 Relationship between strain and depth below the base of footing.

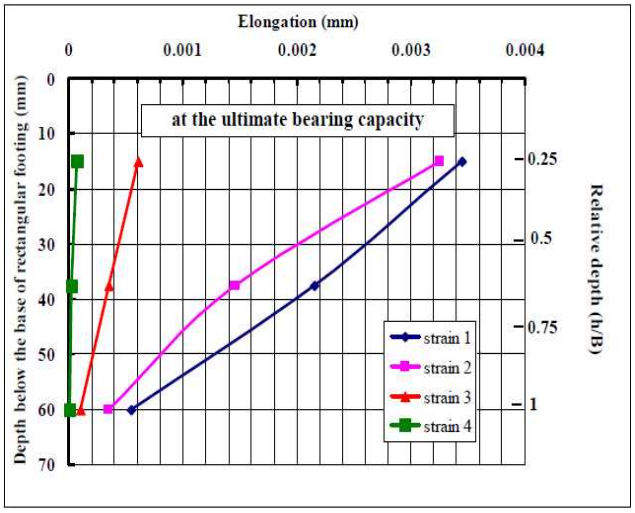

Fig. 13 Relationship between elongation and depth below the base of footing.

5 CONCLUSIONS

The experimental program involved bearing capacity tests using rectangular footing model, with length to breadth ratio of 3.83, resting on sand alone and sand reinforced using three layers of geogrid. A special experimental program was designed to investigate the behavior of strains occurring in the geogrid ribs during the bearing capacity tests, a problem which is not well covered yet. Based on the experimental study the following conclusions may be drawn:

1- The values of bearing capacity improvement ratios (BCR) are 2.9 when using Tensar SS2 and 2.35 when using Netlon CE121 which indicates that the higher the geogrid strength the higher the obtained BCR.
2- At stress equal to the bearing capacity of unreinforced sand, the relative settlement of reinforced sand is smaller than that of unreinforced sand, the improvement in settlement of reinforced sand amounts to 43% and 55% for Netlon CE121 and Tensar SS2 respectively.
3- The relative settlement at failure increases with the increase in (BCR).
4- The effect of the horizontal distance from center line along the long side of footing and the vertical depth underneath footing base is very significant on the strains and elongations occurring in the geogrid ribs.
5- The strain and elongation in the geogrid ribs decrease along the horizontal direction away from center of footing and also decrease in the downward direction underneath footing base.
6- The strain and elongation have practically vanished in the third layer located at depth B beneath the footing.
7- The ribs strains gently decrease in the horizontal direction up to a distance of 1.67B then sharply reduces to insignificant values at a distance of 2.33B after which they gradually dies out at 3.6B which indicates the end of the zone of positive stress.

ACKNOWLEDGEMENT

The work is conducted in the Civil Engineering Departments of Al-Nahrain and Kufa Universities as part of the Ph.D thesis of the third author. The authors would like to express their thanks to all staff of the two departments.

REFERENCES

1) Al-Omari, R. R., Al-Dobaissi, H. H. and Al-wadood, B. A., (1987), "Inextensible Geomesh Included in Sand and Clay", Prediction and Performance in Geotechnical Engineering/Calgary/17-19 June, pp. 155-160.
2) ASTM D422-63, (2007), "Standard Test Method for Particle Size-Analysis of Soils".
3) ASTM D4253-2007, "Standard Test Method for Maximum Index Density and Unit Weight of Soils Using a Vibratory Table".
4) ASTM D4254-2007, "Standard Test Method for Minimum Index Density and Unit Weight of Soils and Calculation of Relative Density".
5) Bergado, D. T., M. Nualkliang, M., Chen, C.T. and Lin, S. S., (2012), "Behavior of Wall/Embankment with Geogrid and Metallic Reinforcements and Verification of K-Stiffness Working Stress Method", International Symposium on Sustainable Geosynthetics and Green Technology for Climate Change (SGCC), 20 to 21 June, Bangkok, Thailand.
6) Chen, Q., (2007), "An Experimental Study on Characteristics and Behavior of Reinforced Soil Foundation", Ph.D. Thesis, University of Louisiana State, USA.
7) Fakhraldin M. K., (2013), "Properties Measurements and Applications of some Geogrids in Sand", PhD Thesis, Alnahrain University.
8) Kolbuszewski, J. J., (1948), "An Experimental Study of the Maximum and Minimum Properties of Sand", Proc. 2nd, ICSM.
9) Pedley, M. J., (1990), "The Performance of Soil Reinforcement in Bending and Shear", Ph.D. Thesis, Oxford University, Britain.
10) Shin E.C. and Das, B.M., (2000), "Experimental Study of bearing Capacity of a Strip Foundation on Geogrid-Reinforced Sand", Journal of Geosynthetics International 2000, VOL. 7, NO. 1, pp. 59-71.